fluids

Review

The Law of the Wall and von Kármán Constant: An Ongoing Controversial Debate

Stefan Heinz

Department of Mathematics and Statistics, University of Wyoming, 1000 E. University Avenue, Laramie, WY 82071, USA; heinz@uwyo.edu

Abstract: The discovery of the law of the wall, the log-law including the von Kármán constant, is seen to be one of the biggest accomplishments of fluid mechanics. However, after more than ninety years, there is still a controversial debate about the validity and universality of the law of the wall. In particular, evidence in favor of a universal log-law was recently questioned by data analyses of the majority of existing direct numerical simulation (DNS) and experimental results, arguing in favor of nonuniversality of the law of the wall. Future progress requires it to resolve this discrepancy: in absence of alternatives, a reliable and universal theory involving the law of the wall is needed to provide essential guideline for the validation of theory, computational methods, and experimental studies of very high Reynolds number flows. This paper presents an analysis of concepts used to derive controversial conclusions. Similar to the analysis of observed variations of the Kolmogorov constant, it is shown that nonuniversality is a consequence of simplified modeling concepts, leading to unrealizable models. Realizability implies universality: there is no need to adjust simplified models to different flows.

Keywords: wall-bounded turbulent flows; law of the wall; von Kármán constant

check for updates

Citation: Heinz, S. The Law of the Wall and von Kármán Constant: An Ongoing Controversial Debate. *Fluids* **2024**, *9*, 63. https://doi.org/10.3390/fluids9030063

Academic Editors: Giuliano De Stefano and Martin Skote

Received: 31 January 2024
Revised: 27 February 2024
Accepted: 29 February 2024
Published: 4 March 2024

1. Introduction

One of the biggest challenges of computational fluid dynamics (CFD) is the reliable and efficient prediction of turbulent flows at high Reynolds number (*Re*), in particular wall-bounded turbulent flows usually seen in reality. Direct numerical simulation (DNS), large eddy simulation (LES), and experimental studies are hardly applicable to extreme *Re* regimes [1], and relatively cost-efficient hybrid RANS-LES, which combine LES with Reynolds-averaged Navier-Stokes (RANS) equations, suffer from reliability issues [2]. There are very promising new developments as given by minimal error hybrid-RANS-LES (which can act as resolving LES) [2–7], but these methods also need evidence for their validity at high *Re*. A closely related challenge is the understanding of the nature of turbulent flow in the limit of infinite *Re*.

The discovery of the law of the wall, the log-law including the von Kármán constant [8], is of essential relevance in this regard. In particular, a proven universal law of the wall has unique practical benefits which cannot be provided in any other way:

B1. It can be used to overcome a very essential problem: it can provide strict guideline for the validation of experiments and computational simulation methods such as DNS, LES, and hybrid RANS-LES for at least several canonical high *Re* flows [9–11].
B2. More specifically, minimal error hybrid RANS-LES were developed recently [2,4–7]. These methods overcome resolution limitations of existing methods, which offers huge computational cost advantages. A universal law of the wall can provide evidence for the validity of such predictions at very high *Re*.
B3. Usually applied turbulence models are developed on the basis of empirical notions. A universal law of the wall can be applied for the design of exact turbulence models. This was demonstrated recently by the derivation of an exact transport equation

for the turbulent viscosity [12]. Such equations can support (not support) empirical turbulence models.

B4. A theory involving a universal law of the wall can essentially contribute to our understanding of the structure of turbulent flows at high *Re* [13]. It can explain *Re* requirements to observe the log-law, the structure of self-similar turbulence characteristics, and convergence toward these structures. Such understanding provides a valuable reference for other turbulent flow studies.

However, after more than ninety years, there is still debate about the validity and universality of the law of the wall. The specific question is whether the mean streamwise velocity U^+ of at least several canonical wall-bounded flows is characterized by log-law variations in absence of boundary effects, this means whether we have $U^+ = \kappa^{-1} ln\, y^+ + B$ including the same von Kármán constant κ and constant B. The superscript $+$ refers to inner scaling; we use $U^+ = U/u_\tau$ and $y^+ = Re_\tau y$ for the inner scaling wall distance, where y is normalized by δ which is the half-channel height, pipe radius, or 99% boundary layer thickness with respect to channel flow, pipe flow, and the zero-pressure gradient turbulent boundary layer (TBL), respectively (the zero-pressure gradient TBL will be referred to simply as TBL). The friction Reynolds number is defined by $Re_\tau = u_\tau \delta/\nu$, where u_τ is the friction velocity and ν is the constant kinematic viscosity.

Figure 1 illustrates the steadily growing interest in these questions with about 1000 journal publications per year right now. The development of views over 80 years [14–41] were reviewed, for example, by Örlü et al. [42], Marusic et al. [43], Smits et al. [44], and Jiménez [45]. The Princeton superpipe (PSP) measurements (involving data up to $Re_\tau = 530{,}023$) were available at this time [46], but concerns about the data accuracy still exist [47]. Supported by increasing access to high *Re* data, the controversial debate of the validity and universality of the law of the wall vibrantly continuous over the last 15 years: traditional views in favor of universality are challenged by opposite views [48–65]. Recent analyses in favor of universality were presented, e.g., in Refs. [56,66–70]. In particular, a comprehensive analysis of available numerical and experimental data up to very high *Re* was presented recently based on observational physics criteria [9,10]. The latter results were recently questioned by data analyses of the majority of existing DNS and experimental results, arguing in favor of nonuniversality of the law of the wall [47,57,71–73].

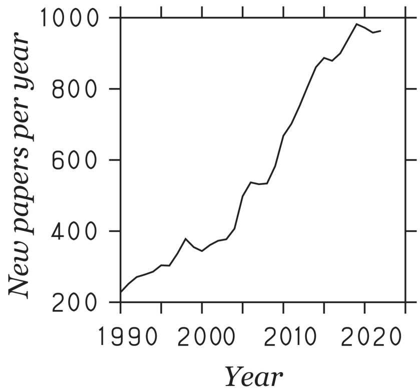

Figure 1. New journal publications per year that mention "law of the wall" and Kármán.

The motivation for this paper is to contribute to the clarification of these questions by an identification of reasons leading to opposite conclusions regarding the universality of the law of the wall and von Kármán constant. The latter clearly matters: this is simply about whether or not there is a reliable universal theory involving the law of the wall which can be used (in absence of alternatives) to validate methods restricted by resolution requirements which are hard to satisfy for very high *Re* turbulent flows. The approach to address these questions is to compare recent analysis results in favor of nonuniversality of the law of the wall [47,57,71–73] with consequences of observational physics criteria [9,10] in the following. The frame of this discussion is illustrated in Table 1: the physical completeness of models is discussed in conjunction with implications for the model realizability and conclusions about universality. In regard to the model realizability, emphasis will be placed on whether or not the methods considered satisfy Reynolds stress-realizability constraints [1,2,74] and realizability constraints arising from the entropy concept. The latter implies the need that the entropy of physically equivalent flows needs to be the same [9,10].

Table 1. Conceptual features of models considered (MN refers to the model of Monkewitz and Nagib [73]).

Model	**Concept**	**Physics**	**Universality**
PVM [9,10]	Physics derived via observational analysis	Realizable model	Universal κ (3 canonical flows)
Cantwell [47]	Neglect of self-similarity (entropy) scaling	Unrealizable entropy	Different κ for every Re & flow
MN [73]	Highly simplified outer-scale model	Unrealizable stress	Different κ for every flow

2. Universal Velocity Models

A probabilistic velocity model (PVM) was introduced in Refs. [9,10] for $Re_\tau \geq 500$ for turbulent channel flow, pipe flow, and the TBL. The model is provided in Table 2, and a discussion of its mathematical structure can be found in the Appendix A. The model was carefully validated against several observational physics requirements, including evidence that both modeled variables and their relevant derivatives accurately represent corresponding observations in regard to all relevant scalings. The model is supported by a probabilistic interpretation: the probability density function (PDF) related to the distribution function for the distribution of mean velocities along the wall-normal direction represents a statistically most-likely PDF that maximizes the related entropy [9,10]. The von Kármán constant κ involved represents an entropy measure.

Table 2. The analytical PVM model valid for $Re_\tau \geq 500$ [9,10]. Here, $B_G()$ refers to the incomplete beta function with subscript G, and $(\cdots, \cdots, \cdots)$ refers to channel flow, pipe flow, and TBL. Corresponding Reynolds shear stress models are given via the momentum balance $S^+ - \langle u'v' \rangle^+ = M$. Here, M refers to the total stress given by $M = (M_{CP}, M_{CP}, M_{BL})$ used in conjunction with $M_{CP} = 1 - y$ and $M_{BL} = e^{-y^6 - 1.57y^2}$.

$$U^+ = U_1^+ + \frac{1}{\kappa}\, ln\left(\frac{1 + Hy^+/y_\kappa}{w + Ky}\right) \qquad \bullet\ H = \left[\frac{y^+/h_1}{1 + y^+/h_1}\right]^{h_3}, \quad K = (0.933, 0.687, 0.285)$$

- $U_1^+ = a\left[cB_G\left(c + \frac{c}{b}, 1 - \frac{c}{b}\right) + G^{\frac{c}{b}}(1-G)^{-\frac{c}{b}} - G^{c+\frac{c}{b}}(1-G)^{-\frac{c}{b}}\right], \quad G = \frac{(y^+/a)^{b/c}}{1 + (y^+/a)^{b/c}}$
- $w = (w_{CP}, w_{CP}, w_{BL}), \quad w_{CP} = 0.1(1-y)^2\left[6y^2 + 11y + 10\right], \quad w_{BL} = e^{-y(0.9 + y + 1.09y^2)}$

$$S^+ = S_1^+ + S_2^+ + S_3^+ + S_1^{CP} + S_2^{CP}$$

- $S_1^+ = 1 - \left[\frac{(y^+/a)^{b/c}}{1 + (y^+/a)^{b/c}}\right]^c, \quad \kappa y^+ S_2^+ = \frac{1 + h_3/[1 + y^+/h_1]}{1 + y_\kappa/(y^+ H)}, \quad \kappa y^+ S_3^+ = -\frac{1 + w'/K}{1 + w/(Ky)}$
- $S_1^{CP} = -yS_1^+(1)\frac{1 - S_1^+}{1 - S_1^+(1)}, \quad S_2^{CP} = -yS_2^+\left(1 - \left[\kappa Re_\tau S_2^+(1)\right]^{-1}\right)$

- $\kappa = 0.40,\ y_\kappa = 75.8,\ a = 9,\ b = 3.04,\ c = 1.4,\ h_1 = 12.36,\ h_3 = 6.47.$

Figure 2 explains the PVM structure. The model involves the contributions S_1^+, S_2^+, and S_3^+ to the characteristic shear rate $S^+ = \partial U^+/\partial y^+$. These shear rate contributions imply corresponding velocity contributions U_1^+, U_2^+, and U_3^+. The inner scaling contributions S_1^+ and S_2^+ (which are only functions of y^+) are the same for all three flows considered. The outer scaling contribution $\kappa y^+ S_3^+$ (which is only a function of y) depends on the flow geometry. There are two inner scale correction terms S_1^{CP} and S_2^{CP} which ensure the correct shear rate limit at the centerline for channel and pipe flow. These contributions provide insignificant corresponding contributions to the mean velocity. As may be seen in Figure 2a, the PVM clearly supports the validity and universality of the log-law. In absence of boundary effects, the PVM implies $U^+ = \kappa^{-1} ln\, y^+ + 5.03$ for all the three flows considered, where $\kappa = 0.40$. A relevant conclusion of the PVM is that critical Reynolds numbers for the observation of a strict log-law for channel flow, pipe flow, and the TBL are given by about Re_τ = 20,000, Re_τ = 63,000, and Re_τ = 80,000, respectively. The excellent PVM performance in comparison to DNS and high-*Re* experimental data is illustrated in Figures 3 and 4.

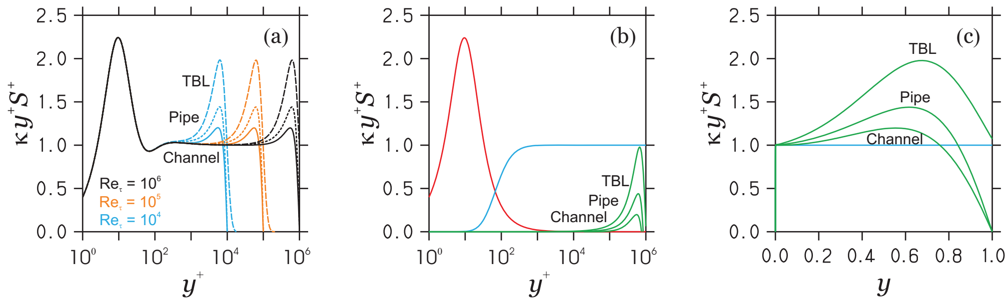

Figure 2. The log-law indicator $\kappa y^+ S^+$ (with $\kappa = 0.4$) obtained from the PVM is shown in (**a**) for the given Re_τ and the three flows considered (channel flow: solid line; pipe flow: short dashes; TBL: long dashes); (**b**) the mode contributions $\kappa y^+ S_1^+$ (red line), $\kappa y^+ S_2^+$ (cyan line), and $\kappa y^+ S_3^+$ (green lines) are shown for $Re_\tau = 10^6$ in inner scaling; (**c**) mode contributions $\kappa y^+ S_2^+$ (cyan line) and $\kappa y^+ (S_2^+ + S_3^+)$ (green lines) are shown for $Re_\tau = 10^6$ in outer scaling. There is no visible $\kappa y^+ S_1^+$ mode.

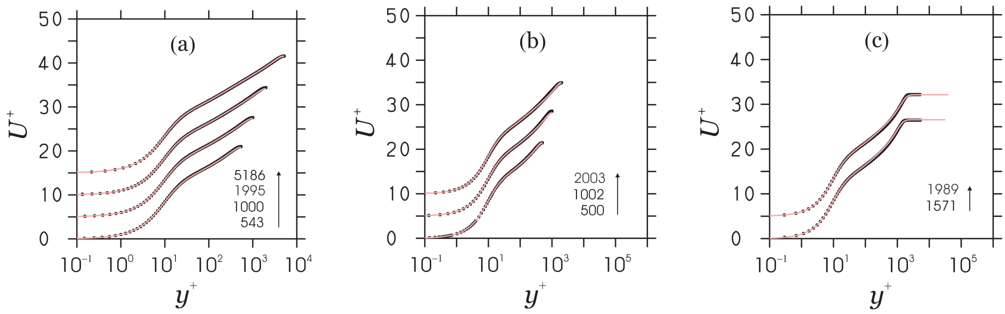

Figure 3. The PVM (lines) compared to DNS data (dots) for the given Re_τ (separated by $\Delta U^+ = 5$). (**a**) Channel flow; DNS data of Lee & Moser [75,76]. (**b**) pipe flow; DNS data of Chin et al. [77]. (**c**) TBL; DNS data of Sillero et al. [78,79].

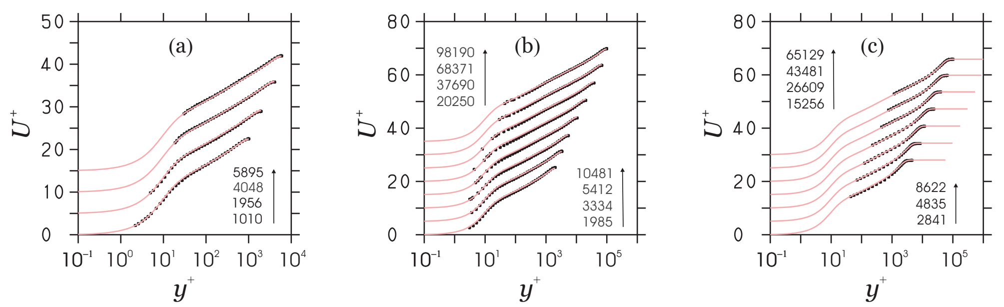

Figure 4. The PVM (lines) compared to experimental data (dots) for the given Re_τ (separated by $\Delta U^+ = 5$). (**a**) Channel flow; experimental data of Schultz & Flack [80]. (**b**) pipe flow; experimental data of Hultmark et al. [81,82]. (**c**) TBL; Pitot experimental data of Vallikivi et al. [83].

There are other models that support the validity and universality of the log-law. One such model is the model of Luchini [56,66]. The characteristic shear rate is described by

$S^+ = 1/(\kappa y^+) + A_1 g/Re_\tau$, where $\kappa = 0.392$, $A_1 = 1$, and $g = (1,2,0)$ for channel flow, pipe flow, and the TBL, respectively. Luchini's model may be seen as basis of the model presented recently by Monkewitz and Nagib (MN) [73]; see the discussion below. The difference is that Luchini does not make an attempt to introduce different von Kármán constants and other constants for different flows considered. Another model that supports the validity and universality of the log-law is the model of Laadhari [68]. The model reads $U^+ = \kappa^{-1} ln(y^*/a)$, where $y^* = y^{+2}S^+$ and $\kappa = 0.40$. This model actually represents an ordinary differential equation (ODE) for U^+. It may be seen that this ODE is solved by $U^+ = \kappa^{-1} ln(y^+/[a\kappa]) = \kappa^{-1} ln(y^+) - \kappa^{-1} ln(a\kappa)$. The setting $a = 0.334$ (which is close to $a = 0.36$ applied by Laadhari [68]) recovers $U^+ = \kappa^{-1} ln\, y^+ + 5.03$ implied by the PVM, i.e., Laadhari's model recovers the implications of the PVM.

A relevant implication of the PVM can be seen by introducing a length scale $\ell = (1 - S_1^+ - S_2^+)^{1/2}/(S_1^+ + S_2^+)$. Figure 5 illustrates the suitability of representing ℓ as $\ell = f_d \kappa y^+$: Figure 5a shows the proportionality to κy^+, Figure 5b shows that $f_d = (1 - S_1^+ - S_2^+)^{1/2}/(S_1^+ + S_2^+)/(\kappa y^+)$ represents a damping function. The definition of ℓ can be used to represent $S_1^+ + S_2^+$ as function of ℓ,

$$(S_1^+ + S_2^+)^{-1} = \left[1 + \sqrt{1 + 4\ell^2}\right]/2. \tag{1}$$

Hence, the length scale ℓ fully determines the flow-independent inner scaling structure of the velocity field. The exact Equation (1) corresponds to an interpolation of limit cases of $S_1^+ + S_2^+ = (1,0)$ for $\ell = (0,\infty)$, respectively. For sufficiently large y^+, Equation (1) implies the log-law $(S_1^+ + S_2^+)^{-1} = \kappa y^+$ because of $f_d = 1$. Via $\ell = f_d \kappa y^+$, it is worth noting that the von Kármán constant κ is the essential ingredient of inner scaling velocity variations.

An additional conclusion on κ is the following. In outer scaling, the PVM provides $y^+ S^+ = [1 + \kappa y^+ S_3^+]/\kappa$ (see Figure 2), so κ can be determined by $y^+ S^+ \to 1/\kappa$ for $y \to 0$. The PVM shows that the contribution of outer scaling variations given by $y^+ S_3^+$ becomes negligible compared to $1/\kappa$ for $y \to 0$ (see Figure 2), i.e., the value of κ is independent of $y^+ S_3^+$ contributions. Hence, κ cannot be determined by the analysis of outer scaling $y^+ S^+$ variations: κ characterizes inner scaling variations (see Equation (1)) which are independent of flow-dependent outer scaling $y^+ S^+$ variations.

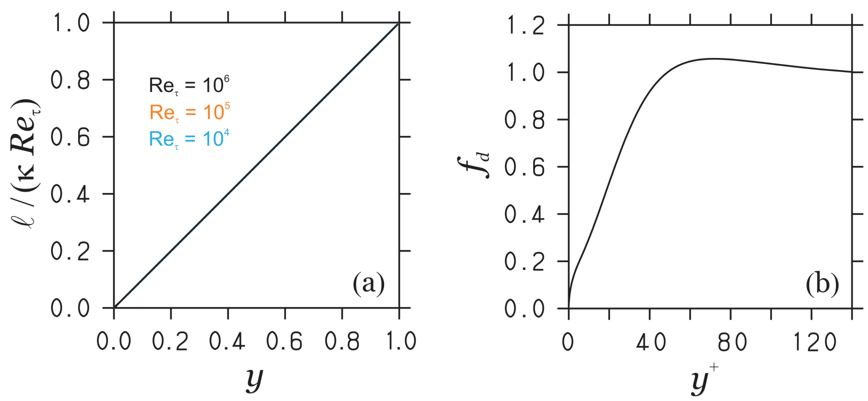

Figure 5. Characteristic features of the length scale $\ell = f_d \kappa y^+$ (**a**) length scale and (**b**) damping function involved.

Used in conjunction with models for the total stress M (see Table 2), we note that the PVM also implies analytical models for the Reynolds shear stress, turbulence production, turbulent viscosity, bulk velocity, skin-friction coefficient, and bulk Reynolds number [9,10]. Asymptotic limits of these variables are reported elsewhere [10]. A closer look at corresponding implications of the PVM for the Reynolds shear stress is beneficial regarding the discussion of nonuniversal velocity models below. By involving ℓ, an asymptotic Reynolds shear stress implied by the PVM for sufficiently high Re_τ is given by

$$-\langle u'v'\rangle_\infty^+ = M\ell^2(S_1^+ + S_2^+)^2, \qquad \ell = f_d\kappa y^+. \tag{2}$$

Hence, $\langle u'v'\rangle^+$ is characterized by self-similar separate variations with y (via M) and with y^+ (via $\ell(S_1^+ + S_2^+)$). As pointed out in Ref. [10], $\langle u'v'\rangle_\infty^+$ approximates $\langle u'v'\rangle^+$ for $Re_\tau = 500$ already extremely well for all three flows considered. For $Re_\tau \geq 10^4$, there is no visible difference between $\langle u'v'\rangle_\infty^+$ and $\langle u'v'\rangle^+$. In particular, the maximum relative deviation between $\langle u'v'\rangle_\infty^+$ and $\langle u'v'\rangle^+$ in percent is given by $E_{uv} = 1355/Re_\tau$ [10]. For $Re_\tau = (10^4, 10^5)$, we find in this way $E_{uv} = (0.14, 0.014)\%$.

3. Nonuniversal Velocity Models

A nonuniversal velocity model was presented recently by Cantwell [47]; see also Ref. [71]. The model uses classical mixing length theory and an ad hoc model for the mixing length λ,

$$-\langle u'v'\rangle^+ = \lambda^2 S^{+2}, \qquad \lambda = \frac{ky^+[1-e^{-(y^+/a)^m}]}{[1+y^n/b^n]^{1/n}}. \tag{3}$$

By using Equation (3) in the momentum equation $S^+ - \langle u'v'\rangle^+ = M$ we can find a model for S^+,

$$S^+ = -\frac{1}{2\lambda^2} + \frac{1}{2\lambda^2}\Big[1 + 4\lambda^2(1-y)\Big]^{1/2}, \tag{4}$$

where $M = 1 - y$ for the pipe flow considered. This model involves five adjustable parameters, k, a, m, b, n, where k corresponds to the von Kármán constant. Figure 15d in Ref. [47] reveals that there is no strict log-law region with the influence of wall and outer length scales on the intermediate region of the velocity profile persisting to all Re_τ [47]. A comparison of model predictions of the normalized turbulent viscosity $\nu_t^+ = -\langle u'v'\rangle^+/S^+$ and turbulence production $P^+ = -\langle u'v'\rangle^+ S^+$ with DNS data and PVM predictions is shown in Figure 6: it may be seen that the model does not accurately reflect the flow structure. An interesting model feature is the following. The y contribution in S^+ is very small for sufficiently high Re_τ, and its influence decreases with increasing Re_τ. For $Re_\tau > 5000$, there is no observable difference anymore between S^+ calculated by Equation (4) and S^+ calculated by neglecting y. In this case, analysis of $dP^+/d\lambda = 0$ shows that the P^+ maximum appears at $\lambda = 2^{1/2}$ (at $S^+ = 1/2$), which provides a maximum $P^+ = 1/4$. A similar PVM analysis leads to a maximum at $\ell = 2^{1/2}$ corresponding to $S_1^+ + S_2^+ = 1/2$ and also $P^+ = 1/4$.

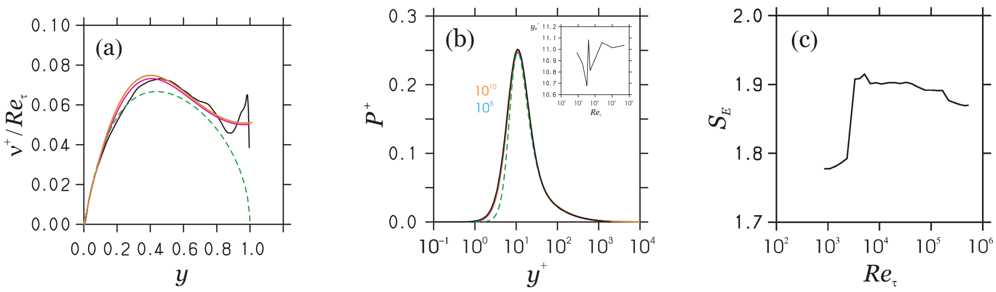

Figure 6. Normalized turbulent viscosity $\nu_t^+ = -\langle u'v'\rangle^+/S^+$ (**a**) and turbulence production $P^+ = -\langle u'v'\rangle^+ S^+$ (**b**) predictions: pipe flow DNS data [77] (black lines), Cantwell model results [47] (dashed green lines, $Re_\tau = 1825$), and PVM results. PVM predictions for $Re_\tau = (2003, 10^5, 10^{10})$ are shown by magenta, cyan, and orange lines. The inset in (**b**) shows production peak positions according to Cantwell's model for the given Re_τ. (**c**) shows the entropy S_E according to Cantwell's model for the given Re_τ.

The nonuniversality of Cantwell's model [47] is reflected by the need to provide k, a, m, b, n (which are determined from an analysis based on the whole velocity profile) as functions of Re_τ. The reason for this nonuniversality is the empirical introduction of Re_τ effects via $y = y^+/Re_\tau$ in λ leading to an unphysical dependence of $\langle u'v' \rangle^+$ on Re_τ. The following provides evidence for this claim.

O1. The simplest way to support this claim is the comparison of Equation (3) with the physics-based Equation (2): although the structures of Equation (2) and (3) are similar, Equation (3) does not ensure a self-similar structure of the Reynolds shear stress in contrast to Equation (2).

O2. The turbulence production peak position is known to be $y^+ = 11.07$, unaffected by Re_τ for sufficiently high Re_τ [9,10]: see Figure 6. For $Re_\tau > 5000$, Cantwell's model provides the production peak position at $\lambda = 2^{1/2}$. According to the definition $\lambda = ky^+[1 - e^{-(y^+/a)^m}]/([1 + y^n/b^n]^{1/n})$ and the Re_τ dependence of model coefficients, this implies y^+ peak positions which vary (randomly) with Re_τ: see the inset in Figure 6b. This behavior is unphysical and in contrast to DNS and experimental results.

O3. More specifically, the model's entropy is given by $S_E = 1 - ln(\kappa) = 1 - ln(k)$ [9]. We find, therefore, random entropy changes for each Re_τ and flow (see Figure 6c). This is unphysical; the entropy needs to be the same under physically equivalent conditions.

Another nonuniversal velocity model was presented recently by Monkewitz and Nagib (MN) [73]. Figure 7 demonstrates the model concept by a comparison with PVM results: MN approximate the log-law indicator y^+S^+ in regard to outer scaling. By following MN, the TBL results are shown in dependence on the boundary layer thickness Y, which differs from the 99% boundary layer thickness [73]. The structure of MN assumptions is illustrated in the insets of Figure 7: linear functions are used to characterize y^+S^+.

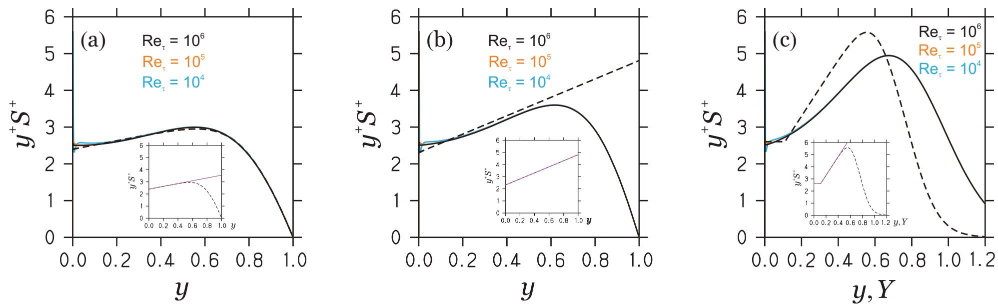

Figure 7. The log-law indicator y^+S^+ in outer scaling obtained by the PVM (solid lines) versus MN assumptions [73] (dashed lines) at the given Re_τ for (**a**) channel flow, (**b**) pipe flow, and (**c**) TBL. For the TBL, the MN assumption is shown depending on the boundary layer thickness Y. Re_τ effects are hardly visible. The insets show the corresponding MN assumptions [73]: y^+S^+ (dashed lines) are shown for $Re_\tau = 10^6$ (there is no Re_τ effect). Also shown are corresponding linear profiles $1/0.417 + 1.15y$, $1/0.433 + 2.5y$, $1/0.384$, and $1/0.384 + 7.7(Y - 0.11)$ (purple lines), respectively.

In regard to MN's model, there seems to be a reasonable agreement between the PVM and MN assumptions. However, a closer look reveals an unphysical model behavior.

O4. MN uses flow-dependent outer scaling y^+S^+ variations (which scale with y) to determine κ based on $y^+S^+ \to 1/\kappa$ for $y \to 0$. However, the PVM reveals that the value of κ is independent of outer scaling y^+S^+ variations (given by $y^+S_3^+$): see the fourth paragraph in Section 2 beginning with "An additional conclusion on κ".

O5. MN presents models for S^+ and $U^+ = \int_0^{y^+} S^+(s)ds$. The MN assumptions imply that both S^+ and U^+ diverge for $y \to 0$ (which is the regime used by MN to determine κ). There is no way to determine κ if the underlying S^+ and U^+ do not exist for $y \to 0$.

O6. Figure 8 shows the correlation of S^+ obtained by the PVM (S^+_{PVM}) and MN (S^+_{MN}). Despite remarkable discrepancies, the most relevant observation is that S^+_{MN} can exceed unity. Combined with the momentum equation $-\langle u'v' \rangle^+ = M - S^+$, we see that the MN model allows values of $-\langle u'v' \rangle^+$ outside $0 \leq -\langle u'v' \rangle^+ \leq 1$, i.e., the MN model violates stress realizability requirements [1,2].

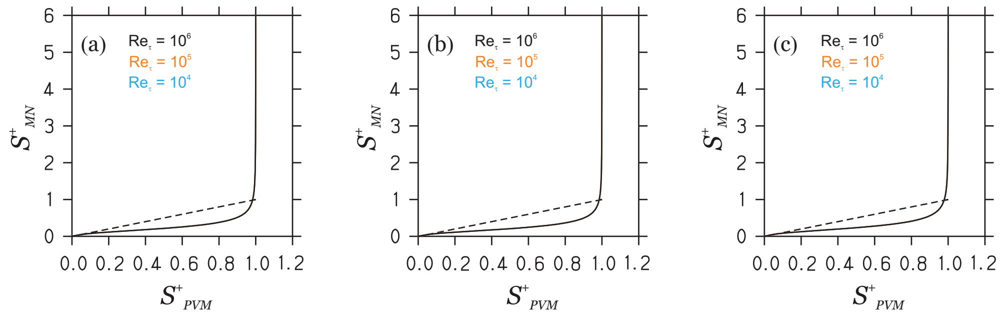

Figure 8. The correlation of S^+ obtained by the PVM (S^+_{PVM}) and MN (S^+_{MN}) is shown for the given Re_τ for (**a**) channel flow, (**b**) pipe flow, and (**c**) TBL. There is no visible Re_τ effect. The dashed lines show the expected 1:1 relationships.

4. Summary

This paper addressed the ongoing controversial debate about the universality or nonuniversality of the law of the wall. The resolution of such controversial conclusions is needed to take advantage of the benefits B1–B4 pointed out in the introduction. According to the observations O1–O6, the conclusion is that observed nonuniversality [47,57,71–73] is a consequence of model assumptions that are in conflict with physics, whereas a universal law of the wall implied by the PVM is found if physics requirements are honored.

More specific lessons learned from this analysis, which are summarized in Table 1, are as follows.

- There is the simple question of which kind of physics a universal law of the wall actually reflects. The PVM gives the answer: the universal log-law is a reflection of a physical entropy and realizable turbulence (a realizable shear stress $\sqrt{-\langle u'v' \rangle^+} = u_*$ which determines a realizable turbulence velocity scale u_*).
- Cantwell's model [47,71] may be seen as a simplification of the PVM, where the self-similarity (entropy) scaling is neglected. It reveals the relevance of the physical entropy requirement: a nonuniversal model reflects an unphysical entropy that is different under physically equivalent conditions; see observation O3.
- MN's model [73] also represents a simplification of the PVM, a highly simplified outer-scale model is used to determine κ. It shows the relevance of the realizability requirement: a nonuniversal model reflects a model that violates the stress-realizability requirement; see observation O6. Such a model cannot reflect reality.

An interesting overall conclusion is as follows. Similar to the von Kármán constant κ, observations of the Kolmogorov constant are affected by significant variations [84]. An analysis of reasons for such variations revealed the influence of model completeness: simplified models that neglect relevant physics provide Kolmogorov constant values that differ significantly from conclusions of physically sound models. A corresponding conclusion was found here in regard to κ: simplified models (Cantwell's model [47,71] and MN's model [73]) that neglect relevant physics (unrealizable models) provide κ values that differ significantly from conclusions of a realizable model (the PVM). Does this mean that a universal velocity model needs to be complicated? This is not the case. As shown in the Appendix A, the PVM is, basically, equivalent to the use of a simple analytical function. In addition to κ, K, y_κ, the PVM only depends on three required regime transition control parameters $(f, H, 1-w)$. The relevant requirement to ensure the universality of the model considered is to honor the regime structure of Equation (A1), which is not the case in regard to the nonuniversal models discussed here.

Funding: This research was funded by the National Science Foundation (AGS, Grant No. 2137351, with N. Anderson as Technical Officer) and support from the Hanse-Wissenschaftskolleg (Delmenhorst, Germany, with M. Kastner as Technical Officer). This work was supported by Wyoming NASA Space Grant Consortium (NASA Grant No. 80NSSC20M0113).

Data Availability Statement: Data are contained within the article.

Conflicts of Interest: The author declares no conflict of interest.

Appendix A. Mathematical PVM Structure

The conclusion about the consequences of simplified modeling approaches obtained here leads to the question about the mathematical structure of the PVM in comparison to simpler modeling approaches. According to Table 2, the PVM can be written as

$$U^+ = U_1^+ + \frac{1}{\kappa} ln\left(\frac{1 + Hy^+/y_\kappa}{w + Ky}\right), \quad U_1^+ = \int_0^{y^+} \Big[1 - f(t)\Big] dt, \quad f(t) = \left[\frac{(t/a)^{b/c}}{1 + (t/a)^{b/c}}\right]^c. \tag{A1}$$

Hence, the PVM is given by a simple analytical function with the exception of the first contribution on the right-hand side (RHS). The exact integration of this expression (U_1^+) provides

$$U_1^+ = \frac{ac}{b}\left[B_G\left(\frac{c}{b}, -\frac{c}{b}\right) - B_G\left(c + \frac{c}{b}, -\frac{c}{b}\right)\right]. \tag{A2}$$

Here, the subscript G in $B_G()$ is defined by $G = (y^+/a)^{b/c}/[1 + (y^+/a)^{b/c}]$. The function $B_G()$ refers to the incomplete beta function, which is defined by

$$B_z(A, B) = \int_0^z s^{A-1}(1-s)^{B-1} ds. \tag{A3}$$

The latter function can be easily calculated by the expansion [85]

$$B_z(A, B) = z^A \sum_{n=0}^{\infty} \frac{p_n z^n}{A + n}. \tag{A4}$$

The last expression introduces p_n, which is defined via $p_0 = 1$ and $p_n = p_{n-1}(n - B)/n$ for $n \geq 1$. Hence, p_n is finite for increasing n. The sum in Equation (A4) is obtained after taking a few terms on the RHS into account. Thus, the PVM calculation via Equation (A1) is, basically, equivalent to the use of a simple analytical function.

According to Table 2, there may be the impression that the PVM has a complicated structure involving a variety of model parameters. A closer look shows the following. In addition to depending on the constants κ, K, y_κ, the PVM only depends on $f, H, 1-w$ (it simplifies the following discussion to take reference to $1-w$ instead of w). Figure A1 shows that these functions are non-decreasing functions varying between zero and unity. Therefore, these functions play the role of distribution functions (i.e., integrals over PDFs), which characterize regime transitions. The same applies to $U_1^+/U_{1\infty}^+$ (where $U_{1\infty}^+ = 15.85$) implied by f, as can be seen in Figure A1a. Correspondingly, in addition to κ, K, y_κ, the PVM only depends on the three required regime transition control parameters $f, H, 1-w$. Appropriate approximations of the latter three functions will hardly affect the model performance. The most relevant requirement to ensure the universality of the model considered is to honor the structure of Equation (A1), which is not the case if the nonuniversal models discussed here are applied.

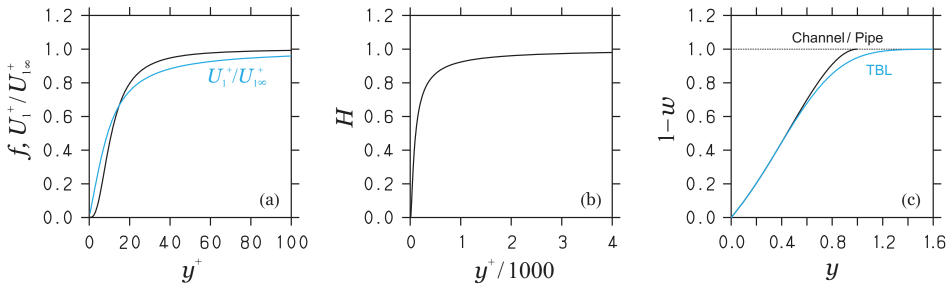

Figure A1. The transition functions f, H, and $1 - w$ are shown in (**a**–**c**), respectively. Figure (**a**) also shows $U_1^+/U_{1\infty}^+$ (blue line). Figure (**c**) also shows $1 - w$ for channel and pipe flow (black line) and the TBL (blue line). The dashed line shows $1 - w = 1$ as a reference.

References

1. Pope, S.B. *Turbulent Flows*; Cambridge University Press: Cambridge, UK, 2000.
2. Heinz, S. A review of hybrid RANS-LES methods for turbulent flows: Concepts and applications. *Prog. Aerosp. Sci.* **2020**, *114*, 100597. [CrossRef]
3. Fagbade, A.; Heinz, S. Continuous eddy simulation vs. resolution-imposing simulation methods for turbulent flows. *Fluids* **2024**, *9*, 22. [CrossRef]
4. Heinz, S. Minimal error partially resolving simulation methods for turbulent flows: A dynamic machine learning approach. *Phys. Fluids* **2022**, *34*, 051705. [CrossRef]
5. Heinz, S. Remarks on Energy Partitioning Control in the PITM Hybrid RANS/LES Method for the Simulation of Turbulent Flows. *Flow Turbul. Combust.* **2022**, *108*, 927–933. [CrossRef]
6. Heinz, S. The Continuous Eddy Simulation Capability of Velocity and Scalar Probability Density Function Equations for Turbulent Flows. *Phys. Fluids* **2021**, *33*, 025107. [CrossRef]
7. Heinz, S.; Mokhtarpoor, R.; Stoellinger, M.K. Theory-Based Reynolds-Averaged Navier-Stokes Equations with Large Eddy Simulation Capability for Separated Turbulent Flow Simulations. *Phys. Fluids* **2020**, *32*, 065102. [CrossRef]
8. von Kármán, T. Mechanische Ähnlichkeit und Turbulenz [Mechanical similitude and turbulence]. In *Nachrichten der Akademie der Wissenschaften Göttingen, Mathematisch-Physikalische Klasse*; Technical Memorandum N611; National Advisory Committee for Aeronautics: Washington, DC, USA, 1930; pp. 58–76.
9. Heinz, S. On mean flow universality of turbulent wall flows. I. High Reynolds number flow analysis. *J. Turbul.* **2018**, *19*, 929–958. [CrossRef]
10. Heinz, S. On mean flow universality of turbulent wall flows. II. Asymptotic flow analysis. *J. Turbul.* **2019**, *20*, 174–193. [CrossRef]
11. Heinz, S.; Heinz, J.; Brant, J.A. Mass Transport in Membrane Systems: Flow Regime Identification by Fourier Analysis. *Fluids* **2022**, *7*, 369. [CrossRef]
12. Plaut, E.; Heinz, S. Exact eddy-viscosity equation for turbulent wall flows—Implications for computational fluid dynamics models. *AIAA J.* **2022**, *60*, 1347–1364. [CrossRef]
13. Heinz, S. The asymptotic structure of canonical wall-bounded turbulent flows. *Fluids* **2024**, *9*, 25. [CrossRef]
14. Millikan, C.B. A critical discussion of turbulent flows in channels and circular tubes. In Proceedings of the 5th International Congress for Applied Mechanics, Cambridge, MA, USA, 22 October 1938; pp. 386–392.
15. Ludwieg, H.; Tillmann, W. Untersuchungen über die Wandschubspannung in turbulenten Reibungsschichten. *Ing. Arch.* **1949**, *17*, 288–299. [CrossRef]
16. Tennekes, H.; Lumley, J.L. *A First Course in Turbulence*; MIT Press: Cambridge, MA, USA, 1972.
17. Hinze, J.O. *Turbulence*, 2nd ed.; McGraw-Hill: New York, NY, USA, 1975.
18. Tritton, D.J. *Physical Fluid Dynamics*; Oxford University Press: New York, NY, USA, 1988.
19. George, W.K.; Castillo, L. Zero-pressure-gradient turbulent boundary layer. *Phys. Rev. Lett.* **1997**, *50*, 689–730. [CrossRef]
20. Zagarola, M.V.; Smits, A.J. Scaling of the mean velocity profile for turbulent pipe flow. *Phys. Rev. Lett.* **1997**, *78*, 239–242. [CrossRef]
21. Barenblatt, G.I.; Chorin, A.J. New perspectives in turbulence: Scaling laws, asymptotics, and intermittency. *SIAM Rev.* **1998**, *40*, 265–291. [CrossRef]
22. Barenblatt, G.I.; Chorin, A.J. Scaling of the intermediate region in wall-bounded turbulence: The power law. *Phys. Fluids* **1998**, *10*, 1043–1044. [CrossRef]
23. Wosnik, M.; Castillo, L.; George, W.K. A theory for turbulent pipe and channel flows. *J. Fluid Mech.* **2000**, *421*, 115–145. [CrossRef]
24. Schlichting, H.; Gersten, K. *Boundary-Layer Theory*, 8th ed.; Springer: Berlin/Heidelberg, Germany, 2000.
25. Barenblatt, G.I. Turbulent boundary layers at very large Reynolds numbers. *Russ. Math. Surv.* **2004**, *59*, 45–62. [CrossRef]
26. Barenblatt, G.I. *Scaling, Self-Similarity and Intermediate Asymptotics*; Cambridge University Press: Cambridge, UK, 1996.

27. Barenblatt, G.I. Scaling laws for fully developed turbulent shear flows. Part 1: Basic hypotheses and analysis. *J. Fluid Mech.* **1993**, *248*, 513–520. [CrossRef]
28. Barenblatt, G.I.; Prostokishin, V.M. Scaling laws for fully developed turbulent shear flows. Part 2: Processing of experimental data. *J. Fluid Mech.* **1993**, *248*, 521–529. [CrossRef]
29. Zagarola, M.V.; Perry, A.E.; Smits, A.J. Log laws or power laws: The scaling in the overlap region. *Phys. Fluids* **1997**, *9*, 2094–2100. [CrossRef]
30. Buschmann, M.H.; el Hak, M.G. Generalized logarithmic law and its consequences. *AIAA J.* **2003**, *41*, 40–48. [CrossRef]
31. Buschmann, M.H.; el Hak, M.G. Debate concerning the mean-velocity profile of a turbulent boundary layer. *AIAA J.* **2003**, *41*, 565–572. [CrossRef]
32. Buschmann, M.H.; el Hak, M.G. Recent developments in scaling of wall-bounded flows. *Prog. Aerosp. Sci.* **2007**, *42*, 419–467. [CrossRef]
33. Buschmann, M.H.; el Hak, M.G. Evidence of nonlogarithmic behavior of turbulent channel and pipe flow. *AIAA J.* **2009**, *47*, 535–541. [CrossRef]
34. Buschmann, M.H.; el Hak, M.G. Turbulent boundary layers: Is the wall falling or merely wobbling? *Acta Mech.* **2011**, *218*, 309–318.
35. Chauhan, K.A.; Nagib, H.M.; Monkewitz, P.A. On the composite logarithmic profile in zero pressure gradient turbulent boundary layers. In Proceedings of the 45th AIAA Aerospace Sciences Meeting and Exhibit, Reno, NV, USA, 8–11 January 2007; p. 07-532.
36. Monkewitz, P.A.; Chauhan, K.A.; Nagib, H.M. Self-consistent high-Reynolds-number asymptotics for zero-pressure-gradient turbulent boundary layers. *Phys. Fluids* **2007**, *19*, 115101. [CrossRef]
37. Nagib, H.M.; Chauhan, K.A. Variations of von Kármán coefficient in canonical flows. *Phys. Fluids* **2008**, *20*, 101518. [CrossRef]
38. Monkewitz, P.A.; Chauhan, K.A.; Nagib, H.M. Comparison of mean flow similarity laws in zero pressure gradient turbulent boundary layers. *Phys. Fluids* **2008**, *20*, 105102. [CrossRef]
39. Chauhan, K.A.; Monkewitz, P.A.; Nagib, H.M. Criteria for assessing experiments in zero pressure gradient boundary layers. *Fluid Dyn. Res.* **2009**, *41*, 021404. [CrossRef]
40. Klewicki, J.; Fife, P.; Wei, T. On the logarithmic mean profile. *J. Fluid Mech.* **2009**, *638*, 73–93. [CrossRef]
41. George, W.K. Is there a universal log law for turbulent wall-bounded flows? *Phil. Trans. R. Soc. A* **2007**, *365*, 789–806. [CrossRef] [PubMed]
42. Örlü, R.; Fransson, J.H.M.; Alfredsson, P.H. On near wall measurements of wall bounded flows–The necessity of an accurate determination of the wall position. *Prog. Aerosp. Sci.* **2010**, *46*, 353–387. [CrossRef]
43. Marusic, I.; McKeon, B.J.; Monkewitz, P.A.; Nagib, H.M.; Smits, A.J.; Sreenivasan, K.R. Wall-bounded turbulent flows at high Reynolds numbers: Recent advances and key issues. *Phys. Fluids* **2010**, *22*, 065103. [CrossRef]
44. Smits, A.J.; McKeon, B.J.; Marusic, I. High-Reynolds number wall turbulence. *Annu. Rev. Fluid Mech.* **2011**, *43*, 353–375. [CrossRef]
45. Jiménez, J. Near-wall turbulence. *Phys. Fluids* **2013**, *25*, 101302. [CrossRef]
46. Zagarola, M.V.; Smits, A.J. Mean-flow scaling of turbulent pipe flow. *J. Fluid Mech.* **1998**, *373*, 33–79. [CrossRef]
47. Cantwell, B.J. A universal velocity profile for smooth wall pipe flow. *J. Fluid Mech.* **2019**, *878*, 834–874. [CrossRef]
48. Baumert, H.Z. Universal equations and constants of turbulent motion. *Phys. Scr.* **2013**, *2013*, 014001. [CrossRef]
49. Wallace, J.M. Highlights from 50 years of turbulent boundary layer research. *J. Turbul.* **2013**, *13*, N53. [CrossRef]
50. Marusic, I.; Monty, J.P.; Hultmark, M.; Smits, A.J. On the logarithmic region in wall turbulence. *J. Fluid Mech.* **2013**, *716*, R3. [CrossRef]
51. Woodcock, J.D.; Marusic, I. The statistical behaviour of attached eddies. *Phys. Fluids* **2015**, *27*, 015104. [CrossRef]
52. Yang, X.I.A.; Marusic, I.; Meneveau, C. Hierarchical random additive process and logarithmic scaling of generalized high order, two-point correlations in turbulent boundary layer flow. *Phys. Rev. Fluids* **2016**, *1*, 024402. [CrossRef]
53. Kazakov, K.A. The mean velocity profile of near-wall turbulent flow: Is there anything in between the logarithmic and power laws? *J. Turbul.* **2016**, *17*, 1015–1047. [CrossRef]
54. Bailey, S.C.C.; Vallikivi, M.; Hultmark, M.; Smits, A.J. Estimating the value of von Kármán's constant in turbulent pipe flow. *J. Fluid Mech.* **2014**, *749*, 79–98. [CrossRef]
55. Wu, Y.; Chen, X.; She, Z.S.; Hussain, F. On the Karman constant in turbulent channel flow. *Phys. Scr.* **2013**, *T155*, 014009. [CrossRef]
56. Luchini, P. Universality of the turbulent velocity profile. *Phys. Rev. Lett.* **2017**, *118*, 224501. [CrossRef]
57. Monkewitz, P.A. Revisiting the quest for a universal log-law and the role of pressure gradient in "canonical" wall-bounded turbulent flows. *Phys. Rev. Fluids* **2017**, *2*, 094602. [CrossRef]
58. Pirozzoli, S.; Smits, A.J. Outer-layer universality of the mean velocity profile in turbulent wall-bounded flows. *Phys. Rev. Fluids* **2023**, *8*, 064607. [CrossRef]
59. Chen, X.; Sreenivasan, K.R. Reynolds number asymptotics of wall-turbulence fluctuations. *J. Fluid Mech.* **2023**, *976*, A21. [CrossRef]
60. Smart, G. A base for the log law and von Karman's constant problem. *J. Hydraul. Res.* **2022**, *60*, 935–943. [CrossRef]
61. Zhang, F.; Zhou, Z.; Zhang, H.; Yang, X. A new single formula for the law of the wall and its application to wall-modeled large-eddy simulation. *Eur. J. Mech. B Fluids* **2022**, *94*, 350–365. [CrossRef]
62. Hansen, C.; Sørensen, J.N.; Yang, X.I.A.; Abkar, M. Extension of the law of the wall exploiting weak similarity of velocity fluctuations in turbulent channels. *Phys. Fluids* **2024**, *36*. [CrossRef]

63. Spalart, P.R.; Abe, H. Empirical scaling laws for wall-bounded turbulence deduced from direct numerical simulations. *Phys. Rev. Fluids* **2021**, *6*, 044604. [CrossRef]
64. Pirozzoli, S. Searching for the log law in open channel flow. *J. Fluid Mech.* **2023**, *971*, A15. [CrossRef]
65. Cheng, W.C. On the value of the von Kármán constant in the atmospheric surface layers over urban surfaces. *J. Wind Eng. Ind. Aerodyn.* **2023**, *241*, 105547. [CrossRef]
66. Luchini, P. Structure and interpolation of the turbulent velocity profile in parallel flow. *Eur. J. Mech. B Fluids* **2018**, *71*, 15–34. [CrossRef]
67. Ali, S.Z.; Dey, S. The law of the wall: A new perspective. *Phys. Fluids* **2020**, *32*, 121401. [CrossRef]
68. Laadhari, F. Refinement of the logarithmic law of the wall. *Phys. Rev. Fluids* **2019**, *4*, 054605. [CrossRef]
69. Epple, P.; Steppert, M.; Malcherek, A. Wall bounded flows and a general proof of the validity of the universal logarithmic law of the wall. In Proceedings of the Fluids Engineering Division Summer Meeting (FEDSM2021) American Society of Mechanical Engineers, Online, 10–12 August 2021; p. FEDSM2021–65733.
70. Guo, J. The log-law of the wall in the overlap from a functional equation. *J. Eng. Mech.* **2023**, *149*, 06022005. [CrossRef]
71. Subrahmanyam, M.A.; Cantwell, B.J.; Alonso, J.J. A universal velocity profile for turbulent wall flows including adverse pressure gradient boundary layers. *J. Fluid Mech.* **2022**, *933*, A16. [CrossRef]
72. Monkewitz, P.A. The late start of the mean velocity overlap log law at—A generic feature of turbulent wall layers in ducts. *J. Fluid Mech.* **2021**, *910*, A45. [CrossRef]
73. Monkewitz, P.A.; Nagib, H.M. The hunt for the Kármán 'constant' revisited. *J. Fluid Mech.* **2023**, *967*, A15. [CrossRef]
74. Heinz, S. Comment on "A dynamic nonlinear subgrid-scale stress model" [Phys. Fluid 17, 035109 (2005)]. *Phys. Fluids* **2005**, *17*, 099101. [CrossRef]
75. Lee, M.; Moser, R.D. Direct numerical simulation of turbulent channel flow up to $Re_\tau = 5200$. *J. Fluid Mech.* **2015**, *774*, 395–415. [CrossRef]
76. 2016. Available online: http://turbulence.ices.utexas.edu (accessed on 1 January 2016).
77. Chin, C.; Monty, J.P.; Ooi, A. Reynolds number effects in DNS of pipe flow and comparison with channels and boundary layers. *Internat. J. Heat Fluid Flow* **2014**, *45*, 33–40. [CrossRef]
78. Sillero, J.A.; Jiménez, J.; Moser, R.D. One-point statistics for turbulent wall-bounded flows at Reynolds numbers up to $\delta^+ \approx 2000$. *Phys. Fluids* **2013**, *25*, 105102. [CrossRef]
79. 2016. Available online: http://torroja.dmt.upm.es/turbdata/blayers (accessed on 1 January 2016).
80. Schultz, M.P.; Flack, K.A. Reynolds-number scaling of turbulent channel flow. *Phys. Fluids* **2013**, *25*, 025104. [CrossRef]
81. Hultmark, M.; Vallikivi, M.; Bailey, S.C.C.; Smits, A.J. Logarithmic scaling of turbulence in smooth-and rough-wall pipe flow. *J. Fluid Mech.* **2013**, *728*, 376–395. [CrossRef]
82. 2016. Available online: https://smits.princeton.edu/superpipe-turbulence-data (accessed on 1 January 2016).
83. Vallikivi, M.; Hultmark, M.; Smits, A.J. Turbulent boundary layer statistics at very high Reynolds number. *J. Fluid Mech.* **2015**, *779*, 371–389. [CrossRef]
84. Heinz, S. On the Kolmogorov constant in stochastic turbulence models. *Phys. Fluids* **2002**, *14*, 4095–4098. [CrossRef]
85. Abramowitz, M.; Stegun, I.A. *Pocketbook of Mathematical Functions–Abridged Edition of Handbook of Mathematical Functions*; JSTOR: New York, NY, USA, 1988.